




Plasma Polymer Deposition of Neutral Agent Carvacrol on a Metallic Surface by Using Dielectric Barrier Discharge Plasma in Ambient Air

Tsegaye Gashaw Getnet^{1,2} , Nilson Cristino da Cruz¹, Milton Eiji Kayama³, and Elidiane Cipriano Rangel¹

¹ Technological Plasmas Laboratory, Paulista State University, Experimental Campus of Sorocaba, Sorocaba, SP, Brazil
tsegshchem2004@gmail.com,

{nilson.cruz, elidiane.rangel}@unesp.br, nilson@sorocaba.unesp.br

² Department of Chemistry, College of Science, Bahir Dar University, Bahir Dar, Ethiopia

³ Laboratory of Plasma and Applications, Sao Paulo State University, Campus of Guaratinguetá, Guaratinguetá, SP, Brazil
milton.kayama@unesp.br

Abstract. This experiment was conducted by newly designed home-made planar type DBD plasma generator in ambient, with industrial argon as the primary plasma-forming and a carrier gas of monomer. Natural agent Carvacrol monomer was used as a precursor in order to deposit plasma polymeric thin film on the surface of metallic material. The discharge characteristics including, the plasma active power, the discharge voltage, and current were diagnosed. The applied voltage was measured by using a voltage divider and the current and the discharge-charge were measured by using the drop of voltage on a resistor and capacitor, respectively. The characteristics of the thin film deposited are presented by varying discharge conditions. The structures of the film, aging, and adhesion were characterized by infrared reflectance spectroscopy and its thicknesses and roughness by profilometry. The obtained thin film was exhibited smooth, dense, uniform, and having chemical similarity to carvacrol monomer. The obtained thin film also exhibited a high thermal resistivity, strong crosslink with good adhesion to the metallic surface. In general, the thin film can be used for practical application as the surface of a biomaterial.

Keywords: Plasma diagnostics · Dielectric barrier discharge · Plasma polymer

1 Introduction

Research in the field of low-pressure plasma has gained emphasis, mainly due to its versatility and the various results obtained in the modification of material physical-chemical properties [1]. However, the large-scale application of low-pressure plasma is mainly limited to the high cost of vacuum installations, and also on the restriction to

not be used in high vapor pressure materials such as living tissues [2, 3]. As a result, several alternative atmospheric or sub-atmospheric pressure plasma techniques, such as corona plasma, microwave, and micro hollow cathode discharge (MHCD), plasma torch and dielectric barrier discharge (DBD) [4, 5], are available nowadays to overcome these limitations since they do not require vacuum systems. Among those various types of plasma sources, DBD atmospheric plasma sources have drawn more attention due to their many advantages, such as low-cost and easy handling and operation [6]. In atmospheric pressure, DBD's can produce diffuse and relatively homogenous non-thermal plasma [7–9]. However, there is a need to improve the stability and repeatability of the discharge for practical and industrial application. In addition to this, as far as our knowledge, there is no study of the atmospheric dielectric discharge plasma of volatile natural agent to produce polymeric films. In this context, the present study was to investigate the use of carvacrol DBD plasma discharge to produce films on the stainless steel surface. This work also deals with the diagnosis of the argon discharge in the presence and absence of carvacrol. We choose stainless steel as a substrate due to its extensive use in many technological applications, consumer products, and biomedical applications.

2 Experimental Device and Operations

2.1 Plasma Diagnosis

In this present study, the dielectric barrier discharge (DBD) equipment was designed and built at the Laboratory of Technological Plasma (LaPTec) of Sao Paulo State University, Brazil. It consists of cylindrical brass with 2 cm in diameter and aluminum disk upper and lower electrodes, respectively. The electrodes were assembled axially with 3 mm gap and hold by circular polyacetal (Delrin) flanges (Fig. 1). The outer surface of the lower electrode was covered by a 0.1 mm thick polyester (Mylar) dielectric sheet. An atomizer with controlled temperature and gas flow rate was used to admixture the gas and the monomer, that was injected through an axial hole in the upper electrode. Argon gas was used because with ambient air in the gap it was not possible to produced filamentary discharge. The output of a neon lamp transformer with 15 kV peak-to-peak voltage with the primary controller by a variac, at 60 Hz frequency, was applied on the upper brass electrode, while the lower one was grounded. The voltage was measured with a voltage divider made with an array of $24 \times 330 \text{ k}\Omega$ resistors and $8.1 \text{ k}\Omega$ load resistor, all connected in series. The current $i(t)$ of the discharge was measured through the voltage drop on a resistor with resistance $R = 57 \Omega$ connected between the lower electrode and the ground. The resistor was replaced by the capacitor $C = 10 \text{ nF}$ to measure the charge produced by the discharge. The signals were displayed and recorded using a 30 MHz and 500 MS/s resolution of two channel digital storage oscilloscope Tektronix TDS 1001C-30EDU to calculate the active power as follows:

$$P_R = \frac{1}{T} \int_t^{t+T} v_A i dt, v_A \gg v_R \quad (1)$$

$$P_C = \frac{1}{T} \int_0^Q v_A dq, v_A \gg v_C \quad (2)$$

where v_A is the applied voltage, v_R the voltage on the resistor, v_C the voltage on the capacitor, T the period, Q the charge in one period in the capacitor and q its instantaneous charge.

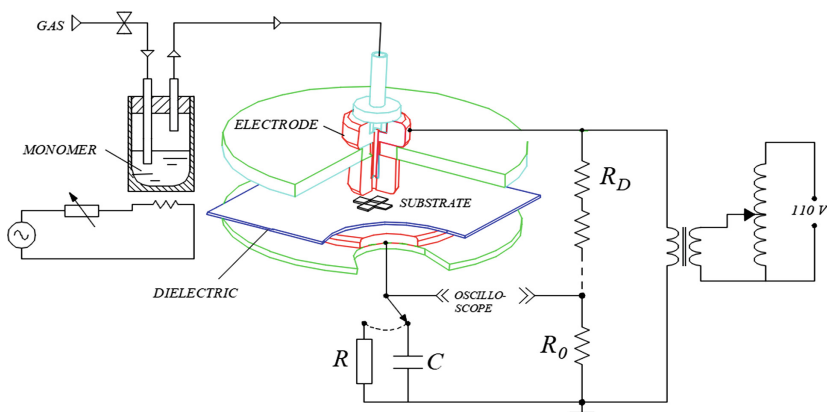


Fig. 1. Schematic representation of the experimental setup.

The chemical structure, aging, adhesion, and thermal resistivity of the films were evaluated by infrared reflectance absorbance spectroscopy (IRRAS), using a Jasco FTIR 410 spectrometer and co-adding 128 spectra with a resolution of 4 cm^{-1} . The thicknesses and roughness of the films were determined with a surface profilometer Veeco Dektak 150.

2.2 Numerical Program

The block diagrams for the numerical calculations of the Eqs. (1) and (2) are shown in the Fig. 2, codes named POWER-VI and LISSA, respectively. They were written to process the digitalized even with high signal to noise ratio. The calculation during one period is repeated as many time as possible on the recorded data. POWER-VI uses a smoothing algorithm for the applied voltage signals maintaining the original current signal. In LISSA, both signals, the applied voltage, and the capacitor voltage are smoothed by different methods. Power is calculated only on well-defined Lissajous figures. Noisy or ambiguous figures are disregarded.

3 Result and Discussion

3.1 Electrical Characteristics

Voltage and Current Waveforms

Figure 3a and b show a typical of the waveform of the current and applied voltage of the discharge of argon without and with carvacrol plasma, respectively. According to the current signal, the DBD plasma discharge worked in filamentary mode consisting

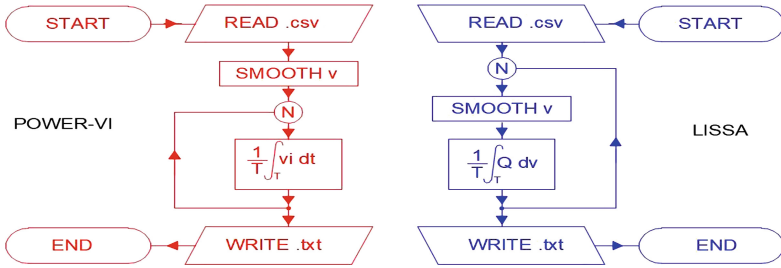


Fig. 2. Block diagrams of the numerical programs

of several micro-discharge channels with a very short time duration corresponding to the peaks on the signal [10]. This is in agreement with the photographic image of the discharge as shown in Fig. 4a and b. There is an augment on the light intensity when we add the monomer in the discharge. It is interesting to point out that the discharge regime of the argon DBD plasma was not altered by the addition of carvacrol monomer and works well for polymer deposition. However, the uniformity and intensity of the discharge are highly affected as we change the amplitude of the applied voltage, the gap of the electrodes and flow rate of the gas. That is when we increase the applied voltage keeping constant flow rate and gap distance, the intensity, and uniformity of the filamentary discharge increase in the gap between the upper electrode and dielectric, as consequence of the increase on the electric field. Similar phenomena were also observed for the increment of the flow rate of the gas. When we increase the gap, more powerful filamentary discharged was produced. On the other hand, when we place the metallic substrate in the gap, as we can see the image of the DBD plasma discharge in Fig. 4c, the discharge concentrates around the substrate. This is due to the distortion of electric field lines promoted by the sharp borders of the substrate.

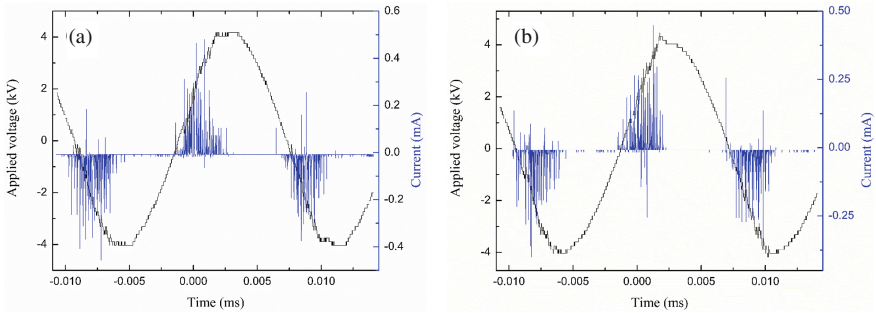


Fig. 3. Voltage and current waveforms of DBD plasma measured at 4.2 kV amplitude applied voltage with a gas flow rate of 5 L/min, (a) Ar only, (b), Ar with carvacrol.

Lissajous Figures

To further analysis of the electrical characteristics, the Q - V plots or the Lissajous figure was studied, as illustrated in Fig. 5. To generate the Lissajous figure, the x-axis is the

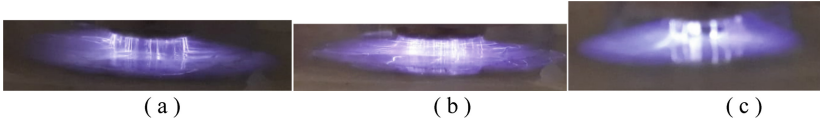


Fig. 4. Images of a DBD plasma discharge at 5.3 kV amplitude applied voltage with 5 L/min flow rate of gas (a), argon only, (b), admixture of argon and carvacrol (c), admixture of argon and carvacrol in the presence of stainless steel disk.

applied voltage in the DBD electrodes, and at the y-axis is the charge in the capacitor $q(t) = C v_C(t)$. Regarding the shape of a Lissajous figure of the DBD filamentary discharge, it looks like a parallelogram as shown in Fig. 5a. In the Lissajous figure, the lines AB and CD represent the phase when no plasma is ignited, while lines DA and BC the phase when the plasma is formed in the gap. The slope of these lines can indicate approximately the total effective capacitance [11]. As we can see in the Lissajous figures, the area of the discharge with argon and carvacrol admixture increases when we place the metallic substrate in the gap, keeping the same remaining discharge condition. It indicates an increase of the plasma active power because of the distortion of electric field lines promoted by the sharp borders of the substrate.

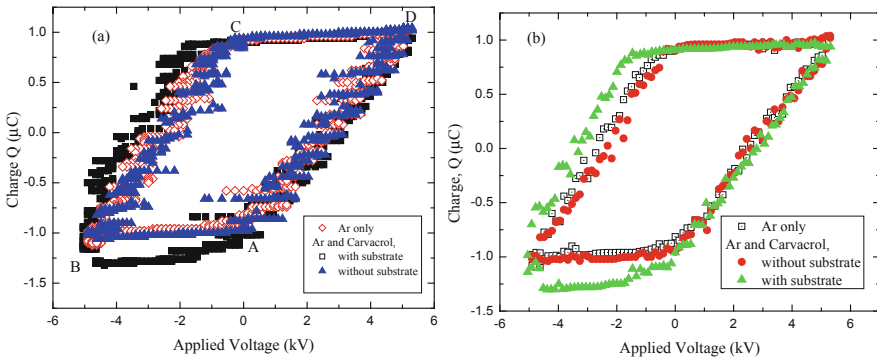


Fig. 5. A Lissajous figure of argon, an admixture of argon and carvacrol in the presence and absence of a substrate in the gap DBD plasma measured at 5.0 kV amplitude applied voltage with a gas flow rate of 5 L/min, (a), raw data, (b), smoothed data.

The active power of discharge in one cycle can be calculated from the area of the Lissajous figure [12]. But in our case, the raw data does not give the exact value of active discharge power, due to the noise in the signal (Fig. 5a). Therefore, a smoothing algorithm was used to obtain the Q - V plots. A typical result of the smoothing process is shown in the Fig. 5b. This reduced data was used to calculate the power according to Eq. 2. Figure 6a and b show the variation of the discharge power of argon only as a function of applied voltage and the gas flow rate, respectively. It is clear that the power increases from 0.4 to 1.4 W, with the applied voltage in the range 4.2–6.6 kV and flow rate of gas between 2 to 6 L/min. Figure 7a and b also shown the power as a function of applied voltage for the admixture of argon and carvacrol in the presence and absence of

a substrate in the gap, respectively. The power calculated by the 57 Ω resistor is higher than the calculated by the capacitor with impedance 2.5 X 10⁵ Ω due to the higher voltage on the discharge for the former.

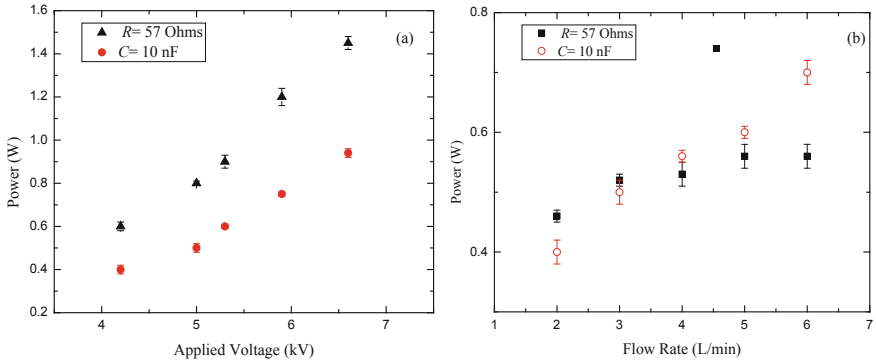


Fig. 6. The variation of the active power of argon DBD plasma at 5 L/min flow rate of gas (a) as a function of applied voltage, (b) as a function of flow rate at 5.3 kV amplitude applied voltage.

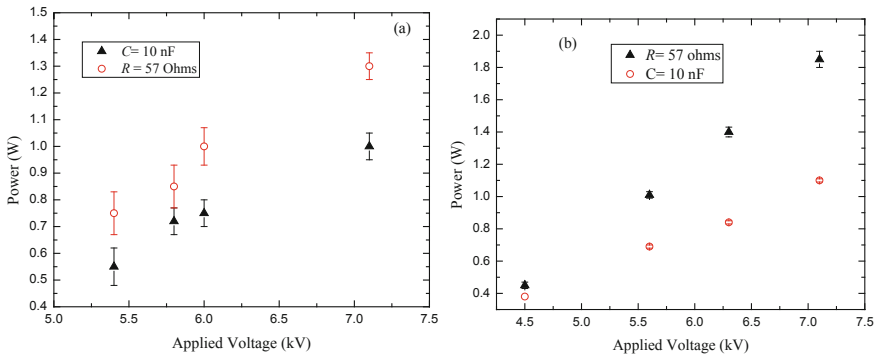


Fig. 7. Relationship between the applied voltage and the produced active power of DBD plasma discharge at 5 L/min flow rate of gas, (a) admixture of argon and carvacrol in presence of substrate (b) admixture of argon and carvacrol.

3.2 Thickness and Rate of Deposition

Polymer thin films were successfully fabricated from carvacrol monomer on both stainless steel and glass slides under different deposition time and applied voltage. Figure 8a and b show the variation of film thickness *h* with deposition time and applied voltage, respectively. The thickness of the film increases from 0.36 to 0.43 μm, with the applied voltage from 3.5 to 6.0 kV. After that, it declines to about 0.32 μm for further increases on the voltage up to 7.5 kV. This is due to the plasma ablation with the overvoltage.

Similarly, the thickness of the film increases with time until 30 min, and decline after this time as shown in Fig. 8b. This decrement of thickness with long disposition time may be attributed to competitive polymerization. The deposition rate also follows the same behaviour of thickness with increasing applied voltage, since the deposition time t is kept constant as shown in Fig. 7a. It is also obvious that the deposition rate increases with deposition time and decline down after a time t . In our case, similar behaviour was also observed as shown in Fig. 7b.

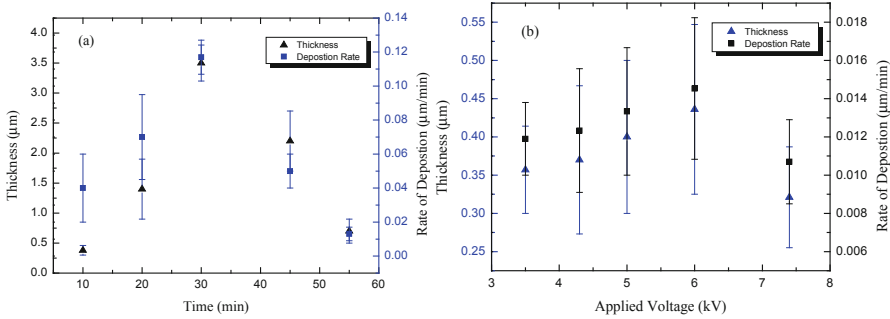


Fig. 8. Thickness and deposition rate of the film at 5 L/min flow rate of gas (a) as a function of time at 7.0 kV (b) as a function of applied voltage at 30 min deposition time.

3.3 Roughness

Figure 9 shows the roughness of the films as a function of active power on the discharge at 10 and 30 min deposition time. The roughness of the film increases with power. At 30 min it has a great deviation due to the creation of holes on the film by the filaments.

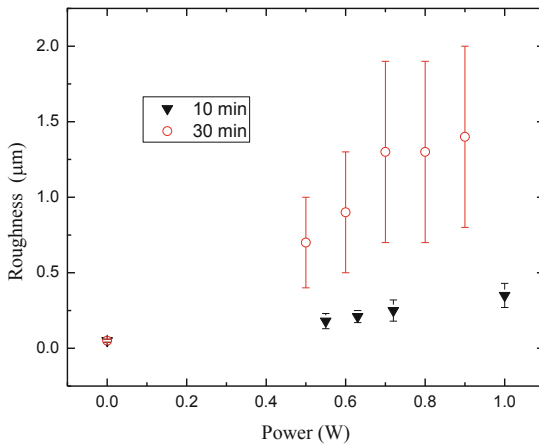


Fig. 9. The roughness of the film as a function of active power at 5 L/min gas flow rate for 10 and 30 min deposition times.

3.4 Chemical Structural Analysis

To complete the structure characterization, FTIR spectra analysis of the monomer (carvacrol) was also carried out in addition to the plasma polymerized carvacrol thin films as shown in Fig. 10a.

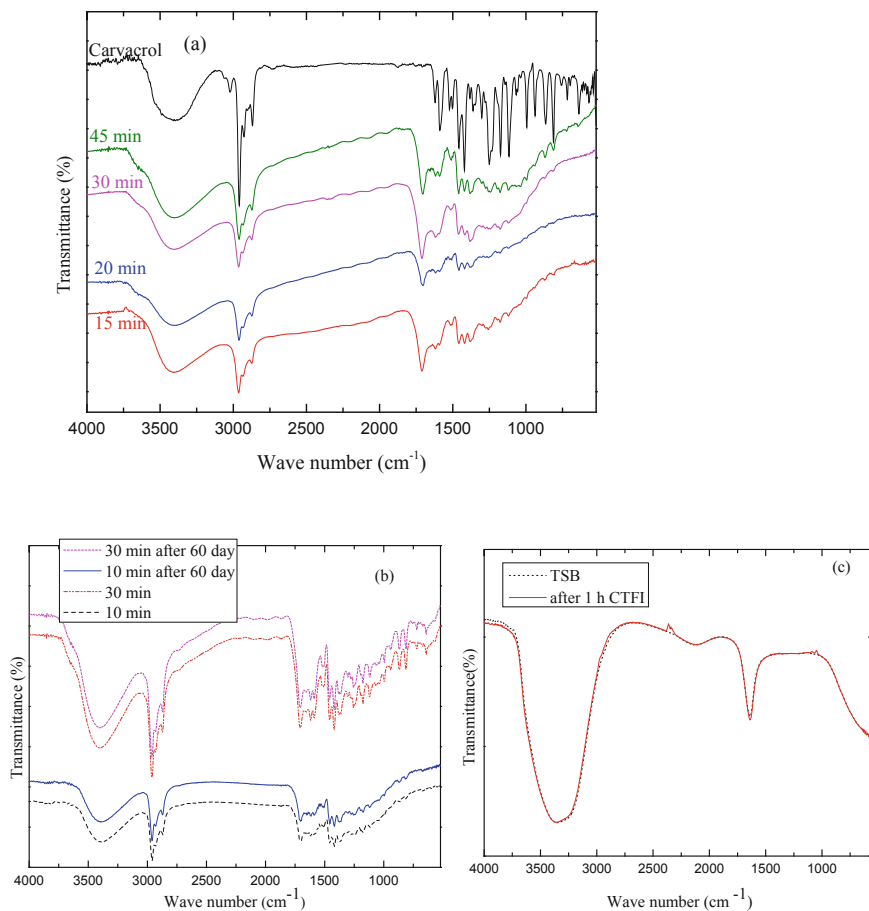


Fig. 10. IR spectra of carvacrol polymer thin film at 0.55 ± 0.06 W active power with 5 L/min flow rate of gas (a) by varying deposition time, (b) after 2 months expose in the air (c) IR spectra of TSB before and 1 h after the immersion of the film. CTFI is carvacrol thin film immersion.

Considering first the spectrum of monomer, a broad peak centered at 3412 cm^{-1} and strong peaks at 1058 and 1112 cm^{-1} shown the O-H and C-O stretching vibration of phenol, respectively. The shorter and strong signals which appeared in the region $3057\text{--}3017\text{ cm}^{-1}$ and $1519\text{--}1620\text{ cm}^{-1}$ showed the presence of aromatic C-H and C = C stretching vibration, respectively. The peaks at 991 , 936 cm^{-1} and 1418 cm^{-1} , also indicated the symmetric and asymmetric in-plane bending of aromatic C-H group (overlapping with the OH bending vibration). Weak bands in the region $862\text{--}808\text{ cm}^{-1}$

and $752\text{--}640\text{ cm}^{-1}$ was due to out of plane bending vibration of adjacent and isolated C-H of 1, 2, 4-substituted benzenoid compounds, respectively. On the other hands, strong absorbance peak in the region of $2959\text{--}2868\text{ cm}^{-1}$ indicate C-H stretch of branched isopropyl [13–16].

When we compare the FTIR spectra of the plasma polymer carvacrol films and of the monomer, the chemical structure was found to be notably similar without the reduction on the intensity of the transmittance peaks, particularly in the fingerprint region. This reduction in the intensity means that a small amount of monomer was polymerized and deposited. When we see the effect of deposition time keeping constant the flow rate, applied voltage and gap distance, the intensity of the peak increases with time. It is in agreement with film thickness referring back Fig. 8a. In general, the FTIR spectrum of all obtained thin films showed the presence of phenols, methyl and aromatic skeletal. It is clearly confirmed the preservation of the monomer functional group upon polymerization.

3.5 Aging and Adhesion of the Thin Film

The thin film aging was examined by using infrared spectroscopy after exposing the film in ambient air for 60 days. The film adhesion also tested by immersing the film in a clean tryptic soy broth (TSB) media for 1 h. As shown in Fig. 10b and c, the IR spectra of the film and TSB were not changed at all. This indicates that the obtained film is highly crosslinked with good adhesion on the surface of the substrate. Therefore, it cannot be easily degraded and removed even in harsh environment.

4 Conclusions

PolyCarvacrol thin film polymerization was successfully deposited by a filamentary dielectric barrier discharge on the metallic surface at different plasma discharge conditions. The surface property of the stainless steel disk was totally changed after treated with carvacrol plasma polymeric thin films. The obtained thin film is also thick, having good adhesion and cannot be aged when exposed to atmospheric air for a long period of time. Finally, the current result encouraging further investigation of carvacrol film coating for biomaterials and food package materials.

Acknowledgments. The authors thank TWAS and CNPq (190896/2015-9) and FAPESP (2012/14708-2) for financial support.

References

1. Alves, C.J., Guerra, C.N., Morais, G.H., Silva, C.F., Hajek, V.: Nitriding of titanium disks and industrial dental implants using hollow cathode discharge. *Surf. Coat. Tech.* **194**(2), 196–202 (2005). <https://doi.org/10.1016/j.surfcoat.2004.10.009>
2. Kanazawa, S., Kogoma, M., Okazaki, S., Moriwaki, T.: Glow plasma treatment at atmospheric pressure for surface modification and film deposition. *Nucl. Instrum. Methods Phys. Res. Sect. B* **37–38**, 842–845 (1989)

3. Yokoyama, T., Kogoma, M., Moriwaki, T., Okazaki, S.: The mechanism of the stabilization of glow plasma at atmospheric pressure. *J. Phys. D Appl. Phys.* **23**(8), 1125–1128 (1990)
4. Napartovich, A.P.: Overview of atmospheric pressure discharges producing no thermal plasma. *Plasmas Polym.* **6**(1), 1–14 (2001)
5. Kayama, M.E., Silva, L.J.S., Vadym, P., Kostov, K.G., Algatti, M.A.: Characteristics of needle-disk electrodes atmospheric pressure discharges applied to modify PET wettability. *IEEE Trans. Plasma Sci.* **45**(5), 843–847 (2017)
6. Laroussi, M., Lu, X., Keidar, M.: Perspective: the physics, diagnostics, and applications of atmospheric pressure low-temperature plasma sources used in plasma medicine. *J. Appl. Phys.* **122**(2), 020901 (2017)
7. Kanazawa, S., Kogoma, M., Moriwaki, T., Okazaki, S.: Stable glow plasma at atmospheric pressure. *J. Phys. D Appl. Phys.* **21**, 838 (1988)
8. Massines, F., Rabehi, A., Decomps, P., Gadri, R.B., Egur, P.S., Mayoux, C.: Experimental and theoretical study of a glow discharge at atmospheric pressure controlled by a dielectric barrier. *J. Appl. Phys.* **82**, 2950–2957 (1998)
9. Yokoyama, T., Kogoma, M., Moriwaki, T., Okazaki, S.: The mechanism of the stabilization of glow plasma at atmospheric pressure. *J. Phys. D Appl. Phys.* **23**, 1125 (1990)
10. Gherardi, N., Gouda, G., Gat, E., Ricard, A., Massines, F.: Transition from glow silent discharge to micro-discharges in nitrogen gas. *Plasma Sources Sci. Technol.* **9**, 340 (2000)
11. Liu, Y., Starostin, S.A., Peeters, F.J.J., Van De Sanden, M.C.M., De Vries, H.W.: Atmospheric-pressure diffuse dielectric barrier discharges in Ar/O₂ gas mixture using 200 kHz/13.56 MHz dual frequency excitation. *J. Phys. D Appl. Phys.* **51**, 11 (2018)
12. Xu, X.: *Gas Discharge Physics*. Fudan University Press, Shanghai (1996)
13. Boughendjioua, H., Djeddi, S., Seridi, R.: A complementary analysis of thyme essential oil by Fourier transformed infrared spectroscopy. *Int. J. Chem. Sci.* **1**(1), 29–32 (2017)
14. Krepker, M., Prinz-Setter, O., Shemesh, R., Vaxman, A., Alperstein, D., Segal, E.: Antimicrobial carvacrol-containing polypropylene films: composition, structure, and function. *Polymers* **10**(1), 79 (2018)
15. Bizuneh, A.: GC-MS and FT-IR analysis of constituents of essential oil from Cinnamon bark growing in South-west of Ethiopia. *Int. J. Herb. Med.* **1**(6), 22–31 (2014)
16. Dias, R.F.: *Organic Chemistry (CHEM311)* Fall 2005, pp. 48–58 (2005)